Segmentation of Human Zygotes in Hoffman Modulation Contrast Images

Alessandro Giusti[a]*, Giorgio Corani[a], Luca Maria Gambardella[a], Maria Cristina Magli[b], Luca Gianaroli[c]

[a]Dalle Molle Institute for Artificial Intelligence (IDSIA) – Manno, Switzerland
[b]International Institute for Reproductive Medicine (IIRM) – Lugano, Switzerland
[c]INFERGEN – Lugano, Switzerland

Abstract. We present a practical graph-based algorithm for segmenting an human zygote (fertilized ovum) in a Hoffman Modulation Contrast image. Such microscopy technique is routinely used during In Vitro Fertilization procedures, and produces an image with a sidelit, 3D-like appearance; our algorithm takes advantage of such peculiar appearance in order to achieve a remarkable robustness in the segmentation task, which is frequently made difficult by clutter, debris and other artifacts. The technique is tested on a number of images with different characteristics, and shown to be robust with respect to clutter, noise and overexposure, and applicable in a wide array of different conditions.

1 Introduction

During In Vitro Fertilization (IVF) procedures, biologists observe fertilized ova at different times in order to assess their quality and select the ones maximizing the implantation success rate; this decision-making process is guided by a number of criteria, usually requiring subjective classifications, which are widely discussed in the related literature [1–3]; Beuchat et al. show in [4] that computer-based morphological measurements on zygotes, providing quantitative rather than qualitative data, has the potential to improve the accuracy of implantation predictions. In this paper we consider the problem of automatically segmenting the zygote cell's oolemma (thus excluding the surrounding zona pellucida, see Figure 1). This allows us to readily compute a number of quantitative measures (apparent size of the cell, simple shape descriptors) which are not easily judged otherwise. The obtained segmentation may also be applied for other tasks, such as driving an automated microscope for unattended imaging of zygotes, or providing a robust, precise initialization for subsequent (automatic or user-assisted) analysis algorithms, such as those introduced in [5, 6].

Our algorithm is designed to operate on Hoffman Modulation Contrast (HMC) images[1]: HMC is an imaging technique converting optical slopes in variations of the light intensity: it is routinely used in IVF labs for observing zygotes, as it provides a large amount of contrast for transparent specimens and eases human observation as the objects appear three-dimensional and side-lit, as if a light source was illuminating them from a side (apparent lighting direction). After using a simple but robust heuristic in order to roughly locate the cell, we compute a transformed representation of the image in polar coordinates; we take advantage of said HMC lighting by only considering edges whose orientation matches the expected sign of the intensity gradient, while penalizing at the same time most unrelated edges. The segmentation problem is finally efficiently solved as a minimum-cost problem on a directed acyclic graph built on the transformed image, which implicitly enforces priors for the cell shape.

*Email: alessandrog@idsia.ch

[1]a technique delivering visually similar results is Differential Interference Contrast (DIC), which is also a likely application scenario for our algorithm

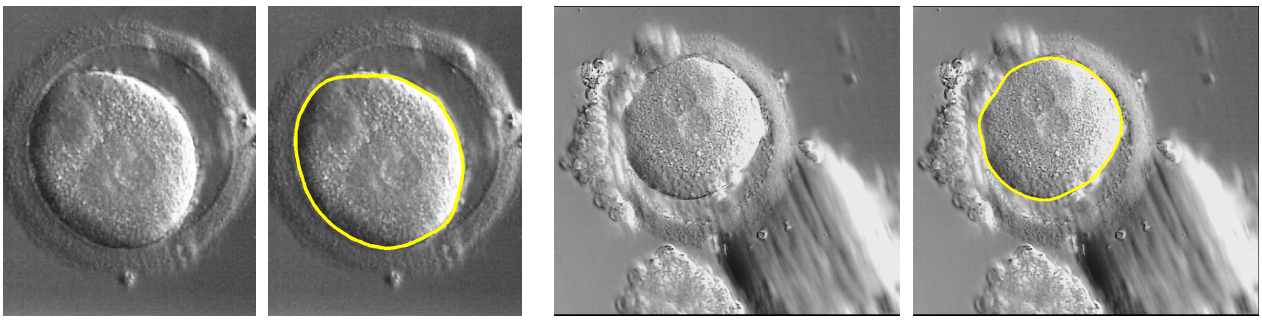

(a) (b) (c) (d)

Figure 1. Zygote cell (a,c) and its segmentation (b,d).

The main contribution of our technique over the state of the art lies in our simple method for taking advantage of HMC lighting, whose effectiveness is quantitatively evaluated in Section 4. The complete system has shown to be remarkably robust and efficient: an image is processed in less than one second, with little effect of debris, noise, overexposure or defocus, and with no need of parameter tuning. This allowed us to easily integrate the technique in the routine of an IVF laboratory, in order to provide precise and effortless zygote measurements.

We briefly review related works in the following Section, then describe our technique in Section 3; experimental results are shown and discussed in Section 4. Section 5 concludes the paper and presents ongoing work.

2 Related Works

Classical region-based segmentation algorithms, including watersheds [7], are not applicable in this context because of the complex appearance of the cell, including the surrounding zona pellucida, clutter, and artifacts; this also hinders the application of straightforward edge-based segmentation algorithms, as many spurious contours are detected.

Iterative energy minimization methods such as active contours [8] and level sets are frequently employed in biomedical imaging: in this context, their application is not straightforward because debris are likely to generate several local minima in the energy function, which makes quick and robust convergence problematic; for example, in [5] active contours are used for measuring the thickness of the zona pellucida in embryo images, but only after a preprocessing step aimed at removing debris and other artifacts.

In [4] a semisupervised technique for measuring various zygote features is used, where the cell shape is approximated by an ellipse: in our case, instead, we recover the actual shape of the cell, which is often not well approximated by an ellipse.

The technique we are presenting includes a global energy minimization step, and may be classified as a specialized graph-cut [9] approach, where: *a)* priors on the cell shape are accounted for by operating on a spatially-transformed image and searching for a minimum-cost path on a directed acyclic graph, and *b)* priors on the contour appearance due to HMC lighting are directly integrated in the energy terms.

Interestingly, several previous works handled the peculiar lighting in HMC and DIC images as an obstacle to segmentation [10], and adopted preprocessing techniques for removing it, whereas we actually exploit such appearance for improving robustness.

3 Segmentation of Zygote Images

We divide the segmentation process in two sequential steps: first, we find the approximate location (c_x, c_y) of the cell center in the original image, which is shot by the biologist while observing a single zygote at a time; then, the image of the cell is transformed to polar coordinates, the lighting parameters are estimated (if unknown), and a shortest-path formulation is used in order to recover the actual zygote contour. We briefly introduce the former part in Section 3.1. The main focus is instead on the latter part, described in Section 3.2.

3.1 Approximate Localization of Zygote Center

In order to find a rough location for the cell centroid, the modulo of the image gradient is first computed at every pixel, then subsampled to a smaller image, which is automatically thesholded and regularized by means of median filtering (see Figure 2 a,b). The largest connected component is isolated and its holes filled (Figure 2 c); for each point inside the resulting region, the minimum distance to the region boundary is computed by means of the distance transform; the point with the maximum distance is finally chosen as the approximate centroid of the cell.

This preliminary analysis phase is not critical for the quality of results, as the subsequent processing tolerates quite large displacements of the detected centroid; nonetheless, this simple algorithm counterintuitively proves to be quite robust also in presence of large artifacts attached to the cell; this is mainly due to the distance transform, which implicitly cancels or reduces the effect of any non-convex artifact protruding off the border of the cell.

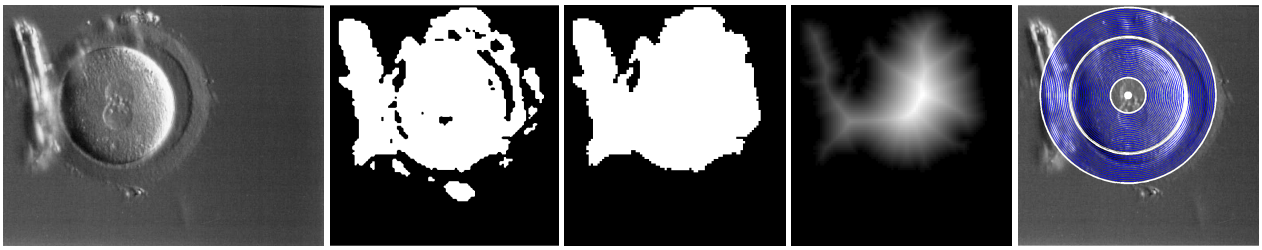

(a) (b) (c) (d) (e)

Figure 2. Approximate localization of the cell center. (a): original image. (b): binary mask obtained after thresholding the modulo of the gradient. (c): largest connected component with holes filled. (d): distance transform. (e) the maximum of the distance transform is considered as the approximate center of the cell. Note that the large artifact on the left does not significantly displace the maximum of the distance transform.

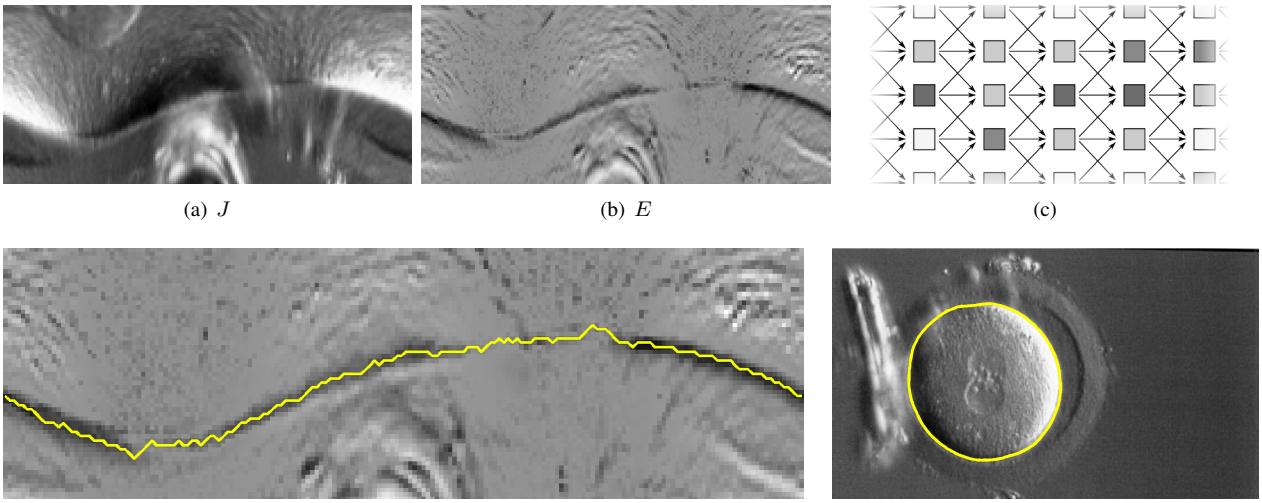

(a) J (b) E (c)

(d) (e)

Figure 3. Contour localization. (a) image in Figure 2 transformed to polar coordinates. (b): energy E computed according to (2), and its graph structure (c). (d): minimum-cost path. (e): the resulting segmentation.

3.2 Detailed Recovery of the Cell Contours

Once the zygote centroid (c_x, c_y) is detected, a circular corona around such point is transformed using bilinear interpolation to an image J in polar coordinates:

$$J(\theta, \rho) = I\left(c_x + \rho\cos(\theta), c_y + \rho\sin(\theta)\right) \qquad 0 \le \theta < 2\pi \quad \rho' \le \rho \le \rho''. \tag{1}$$

In order to account for variations in the cell shape and errors in the centroid location, the range $[\rho', \rho'']$ of ρ values is very conservatively set to $[0.3r, 1.5r]$, where r represents the expected cell radius; this is a quite large range (see Figure 2e), which allows for large variations in the actual radius of the zygote, and for displacements of the estimated centroid (c_x, c_y). ρ and θ values are uniformly sampled in ρ_n and θ_n intervals, respectively, which correspond to rows and columns of image J. We use $\rho_n = 80$, $\theta_n = 180$ in the following.

Image J (Figure 3a) is then processed in order to associate an energy to each pixel, which will drive the following graph-based formulation. Let α be the direction of apparent lighting due to HMC, which only depends on the optical setup and can be assumed known in most scenarios (if it's not, it can be easily estimated); we define the energy for each pixel as:

$$E(\theta, \rho) = P\left(\overbrace{\cos(\theta - \alpha) \cdot G_\rho(J)} + \overbrace{\sin^2(\theta - \alpha) \cdot |G_\rho(J)|}\right) \qquad P(x) = \left(1 + e^{\frac{x}{k}}\right)^{-1} \tag{2}$$

where G_ρ denotes the gradient operator along the ρ axis, and $P(\cdots)$ is a simple decreasing sigmoid function which conditions the energy values to lie in the $[0, 1]$ interval; the scaling parameter k is not critical, and can be safely set to $1/5$ of the image's dynamic range.

The first term in (2) dominates where the contour is orthogonal to the apparent light direction, i.e. where the cell is expected to appear significantly lighter ($\theta - \alpha \simeq 0$) or darker ($\theta - \alpha \simeq \pm\pi$) than the surroundings; large gradient values with a sign consistent with this assumption lead to lower energies. The second term takes account for the unpredictability of the contour appearance where the contour is parallel to the apparent light direction, and just associates lower energies to large absolute values for $G_\rho(J)$.

A directed acyclic graph is built over J, by considering a node for each pixel, and arcs connecting each pixel to its three 8-neighbors at the right (see Figure 3c). The cost of each arc is set to the energy of the source node. The minimum-cost path is computed from every pixel in the first column to the corresponding pixel in the last column; the cheapest of these paths is chosen as the actual contour (see Figure 3d), then mildly smoothed for cosmetic reasons and brought back to cartesian coordinates by using the inverse transform to (1). The interior of the resulting polygon defines the computed binary mask M.

Larger values for ratio θ_n/ρ_n allow more freedom to the path built over J, which translates to better accomodation of an irregular cell shape or a displaced centroid (c_x, c_y); at the same time, this reduces the robustness of the approach, as shape priors are less strongly enforced. We found any ratio between 1.5 and 3 to be acceptable, although we keep with $\theta_n/\rho_n = 180/80 = 2.25$ in the following.

4 Experimental Results

We applied the presented technique to 59 images acquired with a 0.35 megapixel JVC camera attached to an Olympus IX-51 inverted microscope equipped with a 20x objective and HMC. Ground truth is acquired by manually segmenting the zygote in each image, thus obtaining a binary mask T representing the interior of the zygote. The algorithm is implemented in the MATLAB environment equipped with the Image Processing toolbox, and its core functions consist in about 350 lines of code.

For a given computed segmentation, represented by a binary mask M, we consider the Jaccard similarity coefficient as a quality metric, defined by $q = \frac{|T \cap M|}{|T \cup M|}$ $0 \leq q \leq 1$, which approaches 1 for better segmentations. We also measure the average distance d_a and maximum distance d_m between the true boundary and the computed one, as well as the relative error in the measured area e_a, and absolute error in the measured eccentricity e_e.

We evaluate the results obtained by minimizing the energy term E presented in (2). In addition, in order to test the effectiveness of the lighting priors, we also consider two alternative energy terms, which do not include lighting cues:
$E_\rho(\theta, \rho) = P\left(\left|G_\rho\left(J\left(\theta, \rho\right)\right)\right|\right)$, which only considers gradients in the radial direction, without discriminating the sign (i.e. disregarding the expected appearance of the edge); and
$E_G(\theta, \rho) = P\left(\left|G\left(J\left(\theta, \rho\right)\right)\right|\right)$, which considers the gradient magnitude only, disregarding both its sign *and* its direction.

	q	d_a		d_m		e_a	e_e
		pixels	fraction of R	pixels	fraction of R		
E	0.9632	2.6152	0.0201	4.0160	0.0308	0.0133	0.0470
E_ρ	0.9173	6.8304	0.0525	8.4661	0.0651	0.0762	0.0692
E_G	0.8765	11.4302	0.0879	13.3786	0.1029	0.1732	0.0615

Moreover, we stress-tested our technique by simulating variable amounts of additive white gaussian noise, overexposure, and defocus[2] blur (Figure 4 a,b,c).

5 Conclusions

We presented a practical edge-based technique for segmenting the oolemma of the zygote cell, by taking advantage of the peculiar appearance of HMC lighting, which significantly increases the robustness of the system. The algorithm is easily implemented and not computationally expensive, and produces robust, precise results which have been numerically validated.

[2]defocus blur is simulated by convolution with a disk-shaped kernel, which differs from what would occur in a real microscope, where different parts of the cell would come into focus

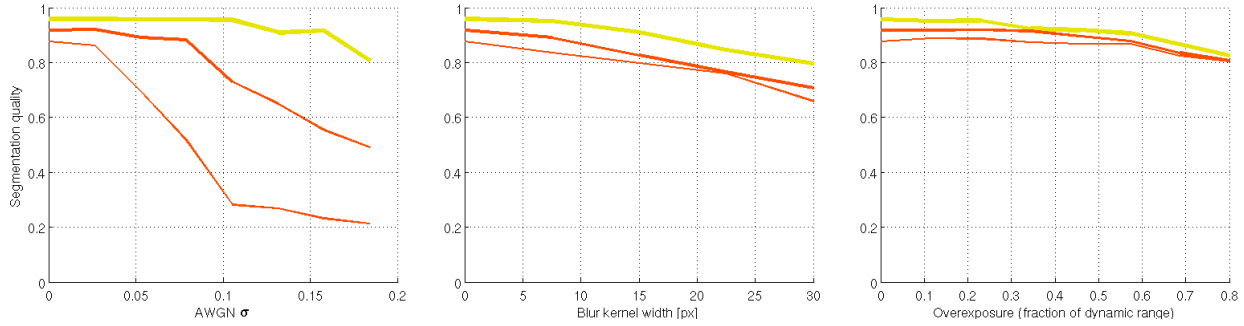

(a) (b) (c)

Figure 4. Average segmentation quality q for the whole dataset, with varying amounts of added noise (a), defocus blur (b) and overexposure (c). Using enegy E (yellow line), E_ρ (thick red line), E_G (thin red).

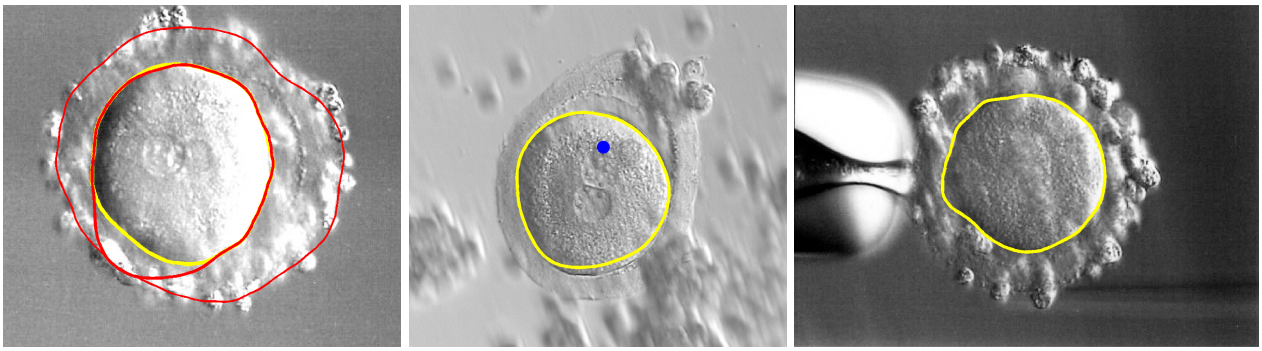

(a) (b) (c)

Figure 5. (a) shows the segmentation obtained using the lighting-aware energy measure E (yellow), versus measures E_ρ (thick red) and E_G (thin red), which are easily misled by artifacts surrounding the cell. (b) shows a failure of our technique (about 15 pixels of error at the bottom of the cell); the failure is due to the recovered approximate cell center (blue dot) being quite displaced. The problem would be solved by either iterating the technique using the center of the computed mask as the new initialization, or by using a larger θ_n/ρ_n ratio. (c) shows our technique working on an ovocyte (not a zygote), which however has a regular enough appearance to be detected and correctly segmented.

The technique is not only useful for directly measuring relevant zygote features: in fact, we are currently using this for automatically initializing iterative techniques for solving more complex problems – such as detection and measurement of pronuclei or zona pellucida – and for automatically detecting the presence of the zygote in the microscope field of view, which is an important prerequisite for unattended zygote imaging within an automated microscopy system.

References

1. T. Baczkowski, R. Kurzawa & W. Głabowski. "Methods of embryo scoring in in vitro fertilization." *Reprod Biol.* 2004.
2. L. Gianaroli, M. C. Magli, A. P. Ferraretti et al. "Oocyte euploidy, pronuclear zygote morphology and embryo chromosomal complement." *Hum Reprod* **22(1)**, pp. 241–249, Jan 2007.
3. M. C. Magli, L. Gianaroli, A. P. Ferraretti et al. "Embryo morphology and development are dependent on the chromosomal complement." *Fertil Steril* **87(3)**, pp. 534–541, Mar 2007.
4. A. Beuchat, P. Thévenaz, M. Unser et al. "Quantitative morphometrical characterization of human pronuclear zygotes." *Hum Reprod* **23**, pp. 1983–1992, 2008.
5. D. Morales, E. Bengoetxea & P. Larrañaga. "Automatic segmentation of zona pellucida in human embryo images applying an active contour model." In *Proc. of MIUA*. 2008.
6. A. Karlsson, N. C. Overgaard & A. Heyden. *Scale Space and PDE Methods in Computer Vision*, chapter A Two-Step Area Based Method for Automatic Tight Segmentation of Zona Pellucida in HMC Images of Human Embryos, pp. 503–514. Springer, 2005.
7. L. Vincent & S. P. "Watersheds in digital spaces: an efficient algorithm based onimmersion simulations." *IEEE Transactions on Pattern Analysis and Machine Intelligence* 1991.
8. C. Xu. "Snakes, shapes, and gradient vector flow." *IEEE Transactions on Image Processing* 1998.
9. R. Zabih & V. Kolmogorov. "Spatially coherent clustering using graph cuts." In *Proc. of CVPR*. 2004.
10. A. Kuijper & B. Heise. "An automatic cell segmentation method for differential interference contrast microscopy." In *Proc. of ICPR*. 2008.